PHYSICAL REVIEW B **70**, 220101(R) (2004)

Local structure and macroscopic properties in $PbMg_{1/3}Nb_{2/3}O_3$-$PbTiO_3$ and $PbZn_{1/3}Nb_{2/3}O_3$-$PbTiO_3$ solid solutions

Ilya Grinberg and Andrew M. Rappe
The Makineni Theoretical Laboratories, Department of Chemistry, University of Pennsylvania, Philadelphia, Pennsylvania 19104-6323, USA

(Received 19 July 2004; published 2 December 2004)

We have examined the local structure of $PbMg_{1/3}Nb_{2/3}O_3$—$PbTiO_3$ (PMN-PT) and $PbZn_{1/3}Nb_{2/3}O_3$—$PbTiO_3$ (PZN-PT) solid solutions using density functional theory. We find that the directions and magnitudes of cation displacement can be explained by an interplay of cation-oxygen bonding, electrostatic dipole-dipole interactions, and short-range direct and through oxygen Pb—*B*-cation repulsive interactions. We find that the Zn ions move off center in the PZN-PT system, which also enables larger Pb and Nb/Ti displacements. The off-centering behavior of Zn lessens Pb—*B*-cation repulsion, leading to relaxor-to-ferroelectric and rhombohedral-to-tetragonal phase transitions at low $PbTiO_3$ content in the PZN-PT system. We also show that a simple quadratic relationship exists between Pb and *B*-cation displacements and the temperature maximum of the dielectric constant, thus linking the enhanced displacements in PZN-PT systems with the higher transition temperatures.

DOI: 10.1103/PhysRevB.70.220101 PACS number(s): 77.80.−e, 71.15.Mb

Heterovalent ferroelectric perovskite solid solutions have been intensively studied[1–5] as they exhibit a range of interesting structural and dielectric properties which make them useful in device applications. Relating the macroscopic properties of these materials to the microscopic properties of the constituent atoms is an important scientific goal and is vital for the rational design of new materials with improved properties. The technologically important[4] $PbMg_{1/3}Nb_{2/3}O_3$—$PbTiO_3$ (PMN-PT) and $PbZn_{1/3}Nb_{2/3}O_3$—$PbTiO_3$ (PZN-PT) solid solutions are good subjects for an investigation of structure-property correlations due to the availability of a wide range of experimental data and because the small difference between Mg and Zn ionic sizes[6] cannot explain the differences in the characteristics of the two solid solutions such as a higher T_c and dielectric constant observed for PZN.[7]

Ab initio density functional theory (DFT) calculations were performed for the $(1-x)$PMN-xPT and $(1-x)$PZN-xPT systems using $2\times2\times2$ 40-atom or $3\times2\times2$ 60-atom supercells with periodic boundary conditions at experimental volume.[7] The energy of the system was evaluated using a local density approximation exchange-correlation functional[8] and was minimized with respect to the atomic coordinates by a quasi-Newton method with no symmetry imposed. A $2\times2\times2$ *k*-point sampling of the Brillouin zone was used. The calculations were done with designed nonlocal norm-conserving pseudopotentials.[9,27] We study four compositions with $x=0$, 0.25, 0.625, and 1.0. For pure PMN and PZN we used a 60-atom supercell with *B* cations arranged according to the random-site model.[10] A *B*-cation arrangement consistent with the random-site model as well as two disordered *B*-cation arrangements were used to model the 0.25 composition and three disordered *B*-cation configurations were used for the 0.625 composition.

The excellent agreement between the pair distribution functions (PDFs) obtained from our relaxed 60-atom structure for PMN and by neutron-scattering experiments[11] (Fig. 1) and similar agreement between DFT and experimental PDFs in previous studies of $PbSc_{2/3}W_{1/3}O_3$—$PbTiO_3$ (PSW-PT), $PbSc_{2/3}W_{1/3}O_3$—$PbZrO_3$ (PSW-PZ),[12] and $PbZr_{1-x}Ti_xO_3$ (PZT) (Refs. 13 and 14) solid solutions indicate that the size of our supercells is sufficient for capturing the local structure of these materials.

We find that at all compositions PZN-PT and PMN-PT local structure is governed by three main interactions. First, bonding interactions with oxygen favor large Pb and *B*-cation displacements (Table I) and creation of short Pb—O and *B*—O bonds. Second, short-range repulsive Pb—*B*-cation interactions create anisotropy in the potential energy surfaces experienced by the Pb cations, leading to a variation in the preferred local displacement direction for the Pb atoms (Table I, Fig. 2). Third, electrostatic interactions favor dipole alignment and tend to minimize the scatter in displacement direction, eliminating displacements opposite to the overall polarization of the supercell (Fig. 2). Breathing motions by the B—O_6 octahedra (to achieve the preferred octahedral volume) and small octahedral rotations (0–5°) are also present.

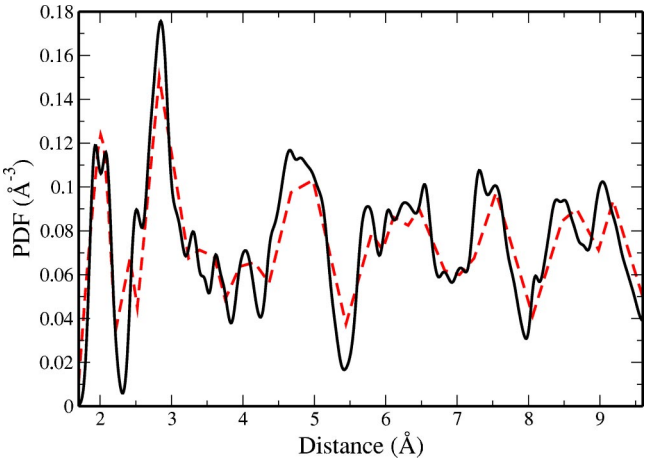

FIG. 1. (Color online) Comparison of PDFs obtained from relaxed structure of 60-atom supercell of PMN (solid, black) and by neutron-scattering (dashed, red) (Ref. 11). Similar agreement is obtained for other systems (Refs. 12 and 14).

TABLE I. Results of DFT calculations for PMN-PT and PZN-PT systems. Pb displacement magnitudes in PMN predicted by DFT are in agreement with recent experimental data (Ref. 25) and P magnitudes for PMN and PT are in good agreement with previous theoretical calculations (Ref. 26). Predicted cation displacements from center of oxygen cage in Å, Pb displacement angle scatter θ_{Pb} in deg, average and local polarization in $\mathrm{C/m^2}$, and experimental $T_{\epsilon,\max}$ (Ref. 7) in K.

	Pb disp.	B^{2+} disp.	Nb/Ti disp.	θ_{Pb}	P_0 av,loc.	$T_{\epsilon,\max}$ expt.
PMN	0.398	0.056	0.168	65	0.38,0.67	276
PMN-0.25PT	0.389	0.080	0.181	33	0.55,0.68	397
PMN-0.625PT	0.387	0.099	0.216	28	0.66,0.74	583
PT	0.440		0.280	0	0.88,0.88	765
PZN	0.444	0.148	0.189	67	0.43,0.73	424
PZN-0.25PT	0.461	0.258	0.205	35	0.66,0.79	547
PZN-0.625PT	0.424	0.270	0.237	27	0.74,0.80	643
PT	0.440		0.280	0	0.88,0.88	765

Examination of the data in Table I shows that for both solid solutions Pb displacement magnitudes predicted by DFT are unchanged by the addition of PT, whereas the average magnitude of the B-cation displacements steadily increases with PT content. The cation displacements are larger in PZN-PT than in PMN-PT, with especially large difference for the B^{2+} cations. While Mg ions are only slightly displaced, the Zn ions exhibit significant distortions even in pure PZN and Ti-like 0.27 Å distortions in Ti-rich PZN-PT. As will be explained later, the large Zn distortions also account for the larger magnitude of Pb, Nb, and Ti distortions in the PZN-PT system.

The contrast between the absence of Mg off-centering and the large Zn displacements is due to the different electronic structure of the two ions. While Mg is a simple metal and

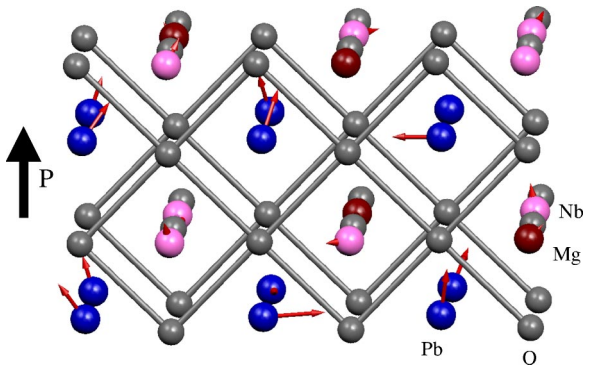

FIG. 2. (Color online) Relaxed structure of 60-atom supercell of PMN obtained by DFT calculations. Cation displacements from high-symmetry positions are shown by arrows scaled up by a factor of 4. Pb atoms displace away from Nb-rich faces. Blue, pink, red, and gray represent Pb, Nb, Mg, and O atoms, respectively. In the black and white version, dark circles in the second and fourth plane from the top are Pb atoms, dark circles in the first and third plane from the top are Mg atoms, light and dark grey represent Nb and O atoms, respectively.

Mg^{2+}—O bonding is essentially ionic, the imperfect screening of the nuclear charge by the d electrons and the presence of low-lying p orbitals make Zn more polarizable and enable covalent bonding with oxygen atoms.[15,16]

As in other Pb-containing ferroelectric perovskite solutions, Pb displacements are the determining factor for the average structure of our solid solutions.[13,14,17] Inspection of Fig. 2 shows that the location of Mg atoms is the primary influence on the direction of Pb distortions. In all cases Pb atoms avoid cube faces with three Nb atoms and one Mg atom and move toward cube faces with two Mg and two Nb atoms. The avoidance of Nb-rich faces is due to the presence of oxygen atoms with two Nb neighbors. Such oxygen atoms have higher B—O bond order than the oxygen atoms in $PbTiO_3$ due to the higher valence of Nb. Since the total bond order of cation-oxygen bonds is conserved at 2, this prohibits the formation of short Pb—O bonds of high bond order and creates a strong effective Pb—Nb repulsive interaction. On the other hand, the oxygen atoms with Mg and Nb neighbors have a lower total B—O bond order than the oxygen atoms in $PbTiO_3$, necessitating the formation of more short Pb—O bonds to compensate for B—O bond depletion[14,18] and leading to a weaker effective Pb—Mg repulsion.

The larger Pb and B-cation displacements in the PZN-PT system are due to the coupling between Zn and Pb and Nb off-center displacements through the Pb—B-cation repulsive interactions. The ionic size of Mg and Zn atoms is essentially the same,[6] which leads to very similar shortest allowed Pb—Mg and Pb—Zn distances. The greater ability of Zn atoms to move off center allows Pb atoms in PZN-PT solution to preserve the required Pb—B-cation distances for larger Pb displacements than in the PMN-PT system. The larger Pb displacements in turn cause larger Nb and Ti distortions to prevent high Pb—B-cation repulsion at short Pb—Nb and Pb—Ti distances.

The electrostatic dipole-dipole interactions favor alignment of cation displacements and prevent cation displacements in the $(\bar{1}00)$ direction in direct opposition to the overall polarization along [100] in Fig. 2. The local direction of Pb displacement is determined by a balance between the need to align with other cation displacements and the need to minimize direct and through-oxygen Pb—B-cation repulsion.[13,14]

At high Ti content, collinear [100] Pb atom distortions create short Pb—O bonds, maximize dipole alignment, and minimize local Pb—B-cation repulsion by avoiding the Ti cations located along the [111] direction. As Ti content decreases, the Pb local environments become anisotropic due to the presence of the overbonded and underbonded oxygen atoms which block Pb distortions toward some [100] perovskite cube faces. This leads to a transition to a rhombohedral phase, where Pb cations move in a variety of low-symmetry directions around the overall [111] polarization direction toward the available low-repulsion cube faces. With the onset of random-site B-cation ordering, the high anisotropy created by a large amount of faces blocked by the presence of overbonded oxygen atoms forbids the formation of a long-range ferroelectric state even in the [111] direction and leads to a relaxor phase. A similar explanation, albeit focused on the

B-cation size difference, for the relaxor-to-ferroelectric transition in the ordered PMN-$PbSc_{1/2}Nb_{1/2}O_3$ system was proposed by Farber and Davies.[19]

While exact Pb-environment population analysis in PMN-PT and PZN-PT is currently not possible due to the complex and unknown nature of the short-range *B*-cation ordering in these systems,[18,20] the above framework coupled with the differences in Zn and Mg distortion behavior explains why in the PZN-PT system the tetragonal phase is present at lower PT content (10%) than in the PMN-PT system (35%), as well as the recent discovery of ferroelectric phases even in pure PZN itself.[21] A large Zn distortion softens Pb—Zn repulsion, making perovskite faces with Zn atoms more friendly toward a Pb distortion than the corresponding perovskite faces with Mg atoms in PMN. This increases the population of the local environments favorable to tetragonal distortion, moving the relaxor-to-ferroelectric transition and the morphotropic phase boundary (MPB) to lower Ti concentrations.

We find that there is also a strong relationship between the low-temperature cation displacements as found by our DFT calculations and the experimentally obtained temperature position of the dielectric constant maximum $T_{\epsilon,\max}$. A qualitative relationship between average lattice displacement and ferroelectric-to-paraelectric phase transition temperature T_c, which is closely linked to $T_{\epsilon,\max}$, was found by Abrahams, Kurtz, and Jamieson (AKJ) in 1968.[22] However, examination of the original AKJ paper shows that the largest discrepancies between predicted and experimental T_c are for the Pb-containing perovskites $PbFe_{1/2}Nb_{1/2}O_3$ and PT. We find that $T_{\epsilon,\max}$ at 1 MHz for PMN-PT, PZN-PT, PZT, $PbSc_{1/2}Nb_{1/2}O_3$ (PSN), PSW-PT, and PSW-PZ solid solutions is predicted by

$$T_{\epsilon,\max} = ad_{\mathrm{Pb}}^2 + bd_{B'}^2 f_{B'}, \tag{1}$$

where d_{Pb} is the average magnitude of the Pb distortions, $d_{B'}$ is the average magnitude of the distortions, $f_{B'}$ is the fraction of the ferroelectrically active *B* cations in solution, and *a* and *b* are constants (1739 and 5961, respectively) in units of $\mathrm{K}/\mathrm{\AA}^2$.

The dependence of $T_{\epsilon,\max}$ on local structure presented in Eq. (1) can be further simplified by transforming cation and oxygen displacements $\mathbf{u}_i$ into 0 K local dipole moments P_{0i} via their Born effective charge tensors $\mathbf{Z}_i^*$.[28] This leads to

$$T_{\epsilon,\max} = \gamma\overline{|P_{0i}|}^2 = \gamma\left(\sum_i \frac{|\mathbf{P}_{0i}|}{N}\right)^2 = \gamma\left(\sum_i \frac{|\mathbf{Z}_i^* \cdot \mathbf{u}_i|}{NV_0}\right)^2 \tag{2}$$

or

$$T_{\epsilon,\max} = \gamma P_0^2 = \gamma\left(\sum_i \frac{\mathbf{P}_{0i}}{N}\right)^2 = \gamma\left(\sum_i \frac{\mathbf{Z}_i^* \cdot \mathbf{u}_i}{NV_0}\right)^2, \tag{3}$$

where γ is a constant, *N* is the number of primitive unit cells, V_0 is the volume of a primitive unit cell, and $\overline{|P_{0i}|}$ and P_0 are the 0 K average magnitude of the local dipole moment and the overall polarization, respectively. Figure 3 shows the correlation between the $T_{\epsilon,\max}$ predicted by Eqs. (1)–(3) and experimental $T_{\epsilon,\max}$ data.[7] The clustering of the data around the $y=x$ line indicates that Eqs. (1)–(3) accurately and quantitatively capture the trends in $T_{\epsilon,\max}$ among these fairly different systems. Comparing the data for PMN-PT and PZN-PT systems in Table I, we see that the higher $T_{\epsilon,\max}$ for PZN-PT system is directly related to larger P_0 and $\overline{|P_{0i}|}$ values due to off-centering behavior on the B^{2+} site.

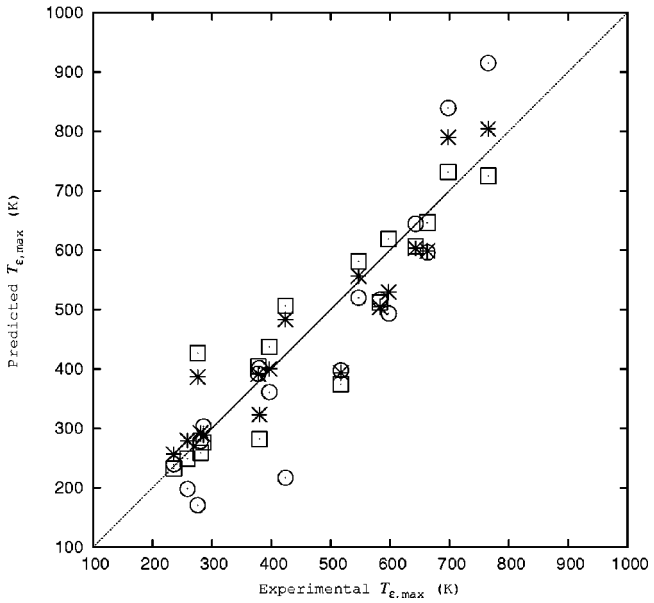

FIG. 3. Correlations between experimental $T_{\epsilon,\max}$ and predicted $T_{\epsilon,\max}$ for PZN, PZN-PT, PMN, PMN-PT, PSW, PSW-PT, PSW-PZ, PSN, and PZT systems. Values for predicted $T_{\epsilon,\max}$ are obtained by Eq. (1) (squares) with $a=1739$ and $b=5961$, Eq. (2) using local polarization with $\gamma=942$ (stars), and Eq. (2) using overall polarization with $\gamma=1189$ (circles).

The correlations presented in Fig. 3 can be explained based on fourth-order Landau theory for ferroelectric crystals. The equilibrium polarization is given by

$$dG/dP = 0 = 2\alpha(T - T_0)P + 4\beta P^3 \tag{4}$$

where α and β are constants, T_0 is the Curie-Weiss temperature at which the dielectric constant ϵ diverges, and *P* is the polarization. Substituting $T=0$ used in our DFT calculations and solving for T_0, we obtain $T_0 = 2\beta P_0^2/\alpha$, thus relating the T_0 to the square of the computed 0 K polarization. The high quality of the fit in Fig. 2 means that for the Pb-based perovskites examined here the ratio β/α is nearly constant.

The energy difference between ferroelectric and paraelectric phases (the ferroelectric instability ΔE_{FE}) is commonly thought to correlate with T_0. However, ΔE_{FE} does not correlate with T_0 for Pb-based perovskites such as PZT,[23] PSW-PT,[12] and $(Cd,Pb)TiO_3$ (CPT).[15,24] The constancy of β/α helps explain this observation. In fourth-order Landau theory ΔE_{FE} at $T=0$ is given by $\Delta E_{\mathrm{FE}} = \alpha^2 T_0^2/4\beta$, with $T_0^2 = (4\beta/\alpha^2)\Delta E_{\mathrm{FE}}$. The β parameter scales the leading order repulsive term and corresponds to the repulsive potential experienced by the off-centering Pb and *B* cations. This potential varies from system to system based on different sizes of the *B* cations.[13,14] Since the ratio of β/α is constant for a wide variety of ferroelectric solutions as shown above, the value of β/α^2 varies. This makes ΔE_{FE} a poor predictor of T_0.

The nearly constant dependence of $T_{\epsilon,\max}$ on P_0^2 and $\overline{|P_{0i}|}$

can be interpreted as follows. Experimental results have shown that ferroelectric-to-paraelectric phase transitions in Pb-based perovskites such as PMN and PZT are of order-disorder character,[25] with Pb displacements at T_0 of up to 70% of the low-temperature value. The parameter governing the temperature of such an order-disorder transition is the coupling strength between the Pb and *B*-cation displacements in neighboring unit cells (corresponding to the *J* parameter in spin models). The coupling is due to electrostatic effects favoring dipole alignment and covalent chemical bonding effects disfavoring under- and overbonded oxygen atoms. Dipole alignment strengths depend only on polarization strengths and gives rise to the overall dependence of T_0 on P_0^2 or $\overline{|P_{0i}|}^2$, with the variation in through-oxygen coupling accounting for the differences between experimental and predicted $T_{\epsilon,\max}$ values in Fig. 3. While predicted $T_{\epsilon,\max}$ values are of the same quality for Eq. (1) and (2), the correlation between P_0 and $T_{\epsilon,\max}$ is somewhat worse. This suggests that the freezing in of large distortions enhances stability of ferroelectricity, giving rise to higher $T_{\epsilon,\max}$. Even though some of the distortions frozen in are not parallel, they still contribute to the coupling of dipoles in neighboring unit cells due to through-oxygen interactions.

In summary, we have examined structure-property correlations for PMN-PT and PZN-PT solid solutions. We find that the local direction of Pb displacements in these systems is governed by an interplay between the electrostatic dipole-dipole alignment interactions and Pb—*B* repulsive interactions, as was previously found for PZT. We find that Zn ions move off center; this reduces Pb—*B* repulsions resulting in smaller Ti content at MPB and allowing larger displacements by the Pb, Nb, and Ti ions. A strong relationship exists between the cation displacements or P_0 and $T_{\epsilon,\max}$, which can be explained in the Landau theory framework by the constant ratio of α and β parameters and is a natural consequence of the order-disorder nature of phase transitions in Pb-based ferroelectrics. The link between α and β also explains the opposite trends in ΔE_{FE} and T_c found in the PZT, PSW-PT, and CPT systems. Fundamentally, we have shown that behavior of individual ions in heterovalent perovskite ferroelectric solid solutions can be directly linked to changes in local structure and macroscopic collective properties.

This work was supported by the Office of Naval Research, under Grant No. N-000014-00-1-0372 and through the Center for Piezoelectrics by Design. We also acknowledge the support of the National Science Foundation, through the MRSEC program, Grant No. DMR00-79909. A.M.R. acknowledges the support of the Camille and Henry Dreyfus Foundation. Computational support was provided by the Center for Piezoelectrics by Design, the DOD HPCMO, and DURIP. We would also like to thank Peter K. Davies for stimulating discussions.

[1] Z.-G. Ye, Curr. Opin. Solid State Mater. Sci. **6**, 35 (2002).
[2] B. Noheda, Curr. Opin. Solid State Mater. Sci. **6**, 27 (2002).
[3] P. M. Gehring, S. Wakimoto, Z. G. Ye, and G. Shirane, Phys. Rev. Lett. **87**, 277601 (2001).
[4] S.-E. Park and T. R. Shrout, J. Appl. Phys. **82**, 1804 (1997).
[5] N. J. Ramer, E. J. Mele, and A. M. Rappe, Ferroelectrics **206**, 31 (1998).
[6] R. D. Shannon and C. T. Prewitt, Acta Crystallogr., Sect. B: Struct. Crystallogr. Cryst. Chem. **26**, 1046 (1970).
[7] T. Mitsui *et al.*, in *Oxides*, Landolt-Bornstein, New Series, Group III, Vol. 16, Pt. a (Springer, Berlin, 1981).
[8] J. P. Perdew and A. Zunger, Phys. Rev. B **23**, 5048 (1981).
[9] N. J. Ramer and A. M. Rappe, Phys. Rev. B **59**, 12471 (1999).
[10] P. K. Davies and M. A. Akbas, J. Phys. Chem. Solids **61**, 159 (2000).
[11] T. Egami, W. Dmowski, M. Akbas, and P. K. Davies, in *First-Principles Calculations for Ferroelectrics*, edited by R. E. Cohen (AIP, Melville, NY, 1998), pp. 1–10.
[12] P. Juhas, I. Grinberg, A. M. Rappe, W. Dmowski, T. Egami, and P. K. Davies, Phys. Rev. B **69**, 214101 (2004).
[13] I. Grinberg, V. R. Cooper, and A. M. Rappe, Nature (London) **419**, 909 (2002).
[14] I. Grinberg, V. R. Cooper, and A. M. Rappe, Phys. Rev. B **69**, 144118 (2004).
[15] S. V. Halilov, M. Fornari, and D. J. Singh, Appl. Phys. Lett. **81**, 3443 (2002).
[16] R. E. Cohen, Nature (London) **358**, 136 (1992).
[17] W. Dmowski, M. A. Akbas, P. K. Davies, and T. Egami, J. Phys. Chem. Solids **61**, 229 (2000).
[18] E. Cockayne and B. P. Burton, Phys. Rev. B **60**, R12542 (1999).
[19] L. Farber and P. K. Davies, J. Am. Ceram. Soc. **86**, 1861 (2003).
[20] B. P. Burton and E. Cockayne, Ferroelectrics **270**, 1359 (2002).
[21] Y.-H. Bing, A. A. Bokov, Z.-G. Ye, B. Noheda, and G. Shirane, cond-mat/0405042 (unpublished).
[22] S. C. Abrahams, S. K. Kurtz, and P. B. Jamieson, Phys. Rev. **172**, 551 (1968).
[23] M. Fornari and D. J. Singh, Phys. Rev. B **63**, 092101 (2001).
[24] D. Y. Suarez-Sandoval and P. K. Davies, Appl. Phys. Lett. **82**, 3215 (2003).
[25] T. Egami, E. Mamontov, W. Dmowski, and S. B. Vakhrushev, in *Fundamental Physics of Ferroelectrics 2003*, edited by P. K. Davies and D. J. Singh (AIP, Melville, NY, 2003), p. 48.
[26] S. A. Prosandeev, E. Cockayne, B. P. Burton, S. Kamba, J. Petzelt, Y. Yuzyuk, R. S. Katiyar, and S. B. Vakhrushev, cond-mat/0404349 (unpublished).
[27] Ionized +2 reference configurations were used for Pb, Mg, and Zn, ionized +4 and +5 were used for Ti and Nb, and a neutral reference configuration was used for O. Energy cutoffs of 50 Ry were used for all elements except for Zn for which 56 Ry was used. Real space cutoffs were 2.0, 1.83, 1.95, 1.70, 1.75, and 1.5 for Pb, Mg, Zn, Ti, Nb, and O, respectively.
[28] Following the approach of Ref. 26, we used approximate Z^* values of 3.6, 2.6, 2.6, 7.4, 4.0, 12.0, 6.4, and 6.4 for Pb, Mg, Zn, Nb, Sc, W, Ti, and Zr, respectively. Oxygen $\mathbf{Z}^*$ were ≈ -5.0 and ≈ -2.5 for the parallel and perpendicular elements of the tensor, respectively, varied slightly to satisfy the electrostatic sum rule for each composition.